

Retrieval of Specific Leaf Area From Landsat-8 Surface Reflectance Data Using Statistical and Physical Models

Abebe Mohammed Ali, Roshanak Darvishzadeh, and Andrew K. Skidmore

Abstract—One of the key traits in the assessment of ecosystem functions is a specific leaf area (SLA). The main aim of this study was to examine the potential of new generation satellite images, such as Landsat-8 imagery, for the retrieval of SLA at regional and global scales. Therefore, both statistical and radiative transfer model (RTM) inversion approaches for estimating SLA from the new Landsat-8 product were evaluated. Field data were collected for 33 sample plots during a field campaign in summer 2013 in the Bavarian Forest National Park, Germany, while Landsat-8 image data concurrent with the time of field campaign were acquired. Estimates of SLA were examined using different Landsat-8 spectral bands, vegetation indices calculated from these bands, and the inversion of a canopy RTM. The RTM inversion was performed utilizing continuous wavelet analysis and a look-up table (LUT) approach. The results were validated using R^2 and the root-mean-square error (RMSE) between the estimated and measured SLA. In general, SLA was estimated accurately by both statistical and RTM inversion approaches. The relationships between measured and estimated SLA using the enhanced vegetation index were strong ($R^2 = 0.77$ and $RMSE = 4.44\%$). Furthermore, the predictive model developed from combination of the wavelet features at 654.5 nm (scale 9) and 2200.5 nm (scale 2) correlated strongly with SLA ($R^2 = 0.79$ and $RMSE = 7.52\%$). The inversion of LUT using a spectral subset consisting of bands 5, 6, and 7 of Landsat-8 ($R^2 = 0.73$ and $RMSE = 5.33\%$) yielded a higher accuracy and precision than any other spectral subset. The findings of this study provide insights into the potential of the new generation of multispectral medium-resolution satellite imagery, such as Landsat-8 and Sentinel-2, for accurate retrieval and mapping of SLA using either statistical or RTM inversion methods.

Index Terms—Landsat-8, radiative transfer model (RTM) and vegetation index (VI), specific leaf area (SLA).

I. INTRODUCTION

SPECIFIC leaf area (SLA), which is defined as the leaf area per unit of dry leaf mass, is an important indicator of plant physiological processes related to ecosystem dynamics. SLA is among the ten essential biodiversity variables proposed by

Manuscript received October 18, 2016; revised January 30, 2017 and March 10, 2017; accepted March 30, 2017. Date of publication April 13, 2017; date of current version August 9, 2017. This work was supported by Netherlands fellowship program. The work of A. M. Ali was supported through the Nuffic Netherlands fellowship program (Nuffic-nfp). (Corresponding author: Abebe Mohammed Ali.)

The authors are with the Faculty of Geo-Information Science and Earth Observation, University of Twente, Enschede 7500, The Netherlands (e-mail: abebemohammed@yahoo.co.uk; r.darvish@utwente.nl; skidmore@itc.nl).

Color versions of one or more of the figures in this paper are available online at <http://ieeexplore.ieee.org>.

Digital Object Identifier 10.1109/JSTARS.2017.2690623

Skidmore *et al.* [1] to capture biodiversity change from space. SLA links plant carbon and water cycles, and provides information on spatial variation of photosynthetic capacity and leaf nitrogen content [2]. Knowledge on SLA values is important in ecosystem function assessments and for understanding plants' growth strategies, especially with respect to climate change. Accurate and regularly repeated SLA estimates at global, regional, and local scales is needed when monitoring ecosystem, as well as for appropriate planning and monitoring of conservation strategies. Therefore, pinpointing affordable, timely, and readily-available remote sensing data together with robust processing techniques are indispensable for fast and cost-effective SLA estimation.

The application of remote sensing for estimating forest variables, such as SLA, has not been demonstrated using satellite-based data. As such, many studies have focused on high spatial and high spectral airborne imagery for the quantification of vegetation parameters in forests, e.g., [3], [4]–[8]. However, the high cost and large data volume associated with airborne data impede the use of airborne imagery for estimating vegetation variables at large spatial scales. The utilization of a new generation of satellites, which allows acquisitions of imagery at medium resolution (i.e., spectral and spatial properties), could be an alternative for accurate retrieval of forest variables including SLA at different spatial scales.

Landsat is widely available medium-resolution satellite sensors providing high temporal imagery for regional, continental, and global vegetation studies. The recently launched Landsat-8 operational land imager (OLI) is one of the medium spectral and spatial resolutions imagery that has global coverage and complemented by the recently launched Sentinel-2. Comparison of Landsat-8 OLI and Landsat-7 enhanced thematic mapper plus (ETM+) data among different vegetation types confirmed that differences in the sensor characteristics of OLI and ETM+ have a little impact on Landsat data continuity [9], [10]. Several studies have been undertaken to estimate vegetation parameters (including biomass and phenology) from Landsat-8 reflectance data by applying either statistical or physical remote-sensing methods, e.g., [8], [11]–[13]. The data (Landsat-8) have been further tested for estimating rice phenology date in China, using the normalized difference vegetation index (NDVI) and enhanced vegetation index (EVI) [14]. Estimation of fraction of absorbed photosynthetically active radiation has been improved when multiple satellite data from MODIS, MISR, Landsat

Thematic Mapper (TM), and ETM+ were used [15]. A review of the literature revealed that Landsat-8 imagery has not been used to estimate SLA. As far as we know, the only study done on SLA estimation from spaceborne imagery was by Lymburner *et al.* [16] using vegetation indices. Previous studies have focused mainly on the retrieval of SLA from hyperspectral (airborne) imagery. These hyperspectral (airborne)-based studies include SLA retrieval using statistical techniques, such as narrow-band vegetation indices [17]–[19] and radiative transfer model (RTM) inversion through continuous wavelet analysis (CWA) [20]. However, estimating vegetation parameters using either statistical or RTM inversion approaches has advantages and disadvantages [21], and the available resources as well as expertise are often the main drivers of model selection.

In this study, our aim was to explore the potential of Landsat-8 data for estimating SLA in a mountain forest. The study benefits from a comprehensive validation dataset acquired during the summer of 2013. Our specific objectives were to 1) create empirical models to relate Landsat-8 reflectance and its derived spectral indices or features to SLA measured on the ground, 2) evaluate Landsat-8 reflectance data through inversion of RTM by using CWA and look-up table (LUT) approaches to estimate SLA, and 3) evaluate whether upscaling through Landsat-8 data would affect the SLA retrieval accuracy and models that others have investigated using airborne hyperspectral data.

II. METHODS

A. Test Site and Field Data

The test site for this study was the mixed mountain forest of the Bavarian Forest National Park. The park is located in southeastern Germany along the border with the Czech Republic (49° 3' 19" N, 13° 12' 9" E central location). Elevation of the test site varies from 600 to 1473 m above sea level. The climate of the region is temperate, with high annual precipitation (1200 to 1800 mm) and low average annual temperature (3–6 °C). Heavy snow cover is characteristic of the area in winter. Brown soils are the predominant soil type at lower altitude (below 900 m a.s.l), whereas at high altitude (above 900 m a.s.l), brown soils and brown podzolic soil predominate. The soils in the area are naturally acidic and low in nutrient content [22].

The natural forest ecosystems of the Bavarian Forest National Park vary with altitude: there are alluvial spruce forests in the valleys, mixed mountain forests on the hillsides, and mountain spruce forests in the high areas. The dominant tree species include European beech (*Fagus sylvatica*), Norway spruce (*Picea abies*), and fir (*Abies alba*). In the mixed mountain forests, sycamore maple (*Acer pseudoplatanus* L), Mountain ash (*Sorbus aucuparia* L), and goat willow (*Salix caprea*) are also found [23]. Due to heavy disturbance by bark beetle and wind storms in recent decades, the forest structure in the park is very heterogeneous [24].

A field campaign was conducted during summer 2013 to collect field data. The test site was stratified into broadleaf, conifer, and mixed forest stands. Given the heterogeneity of the forest and the time and cost constraints, we randomly selected 33 plots from the three main forest class strata, resulting in

ten samples in broadleaf stands, nine in conifer stands, and 14 in mixed stands. Each plot was square, with sides 30 m long. In all 33 sample plots, forest structural variables, such as leaf area index (LAI), stem density (SD), canopy closure (CC), crown diameter (CD), and stand height (SH) were measured. The LAI of each plot was measured using an LAI-2000 canopy analyzer and was also computed from the hemispherical photographs taken in each plot. The SD was recorded as the number of trees per hectare based on the number of trees in each plot. CC was estimated by averaging five observations in a plot using a crown densiometer. CD and SH were calculated from the mean CD and mean height of five randomly selected trees in each plot. The CD of each tree was determined by averaging two perpendicular projected distances on the ground. The total height of each tree was estimated by using a Nikon Forestry 550 laser rangefinder.

In each plot, leaf samples were collected from mature sunlit leaves at the top of the canopy of three to five trees, using a crossbow, and their characteristics were measured. Leaf area of broadleaf samples was measured using the LI-3000C portable leaf area meter (Li-Cor, Inc., Lincoln, NE, USA). The surface of sample conifer needles was scanned using an HP double lamp desktop scanner at a resolution of 1200 dpi; the needle projections were computed from the grayscale images using ImageJ image processing software (which is freely available online); for details on the leaf samples' spectral and physical variable measurements see [25]. The collected leaf samples were transported to the laboratory for further analysis. All samples were oven dried at 65 °C for 48 h and then SLA, leaf mass per leaf area (C_m), and leaf water content (C_w) were computed based on fresh and oven-dried leaf mass and corresponding leaf areas. SLA was computed by dividing oven-dried weight of each sample by its area. The leaf structural parameter (N) was retrieved by inverting the PROSPECT model, using simulation at three wavelengths (see [25]). For mixed plots, the average values for SLA, C_m , C_w , and leaf structural parameter (N) were based on crown biomass proportion of each species in a given plot. The variables measured in the field are summarized in Table I.

During the field campaign, the spectral reflectance of understory vegetation and ecosystem elements on the forest floor, such as bark, litter, mosses, and lichens, was also measured by using the ASD field spectroradiometer coupled to a high-intensity contact probe.

B. Landsat-8 Imagery and Preprocessing

The Landsat-8 observatory operates in a near-circular near-polar sun-synchronous orbit with a 705-km altitude at the equator. The observatory has a 16-day ground track repeat cycle with an equatorial crossing at 10:11 a.m. (± 15 min) mean local time during the descending node. In this orbit, the Landsat-8 observatory follows a sequence of fixed ground tracks (also known as paths) defined by the second worldwide reference system (WRS-2). WRS-2 is a path/row coordinate system used to catalog all the science image data acquired from the Landsat 4–8 satellites. The Landsat-8 launch and initial orbit adjustments placed the observatory in an orbit to ensure an eight-day

TABLE I
SUMMARY STATISTICS OF THE MEASURED AND CALCULATED LEAF PARAMETERS AND CANOPY STRUCTURAL VARIABLES OF THE 33 SAMPLE PLOTS IN THE BAVARIAN FOREST NATIONAL PARK

Parameter	C_m (g/cm ²)	C_w (g/cm ²)	N	SLA (cm ² /g)	LAI (m ² /m ²)	SD (n/ha)	CC (%)	CD (m)	SH (m)	ALA (deg)
Minimum	0.0061	0.0071	1.36	43.45	2.42	222	38	2.91	12.26	40
Maximum	0.0292	0.0309	1.93	165.64	6.18	1722	91	10.55	27.36	60
Mean	0.0147	0.0178	1.58	89.38	4.3	778.4	75.19	5.67	20.23	50
St. dev.	0.0059	0.0071	0.16	37.72	0.81	405.5	5.33	1.56	4.52	9.96

The measured leaf parameters were leaf mass per leaf area (C_m), leaf water content (C_w), and SLA. Leaf structural parameter (N) was estimated using the PROSPECT model. The canopy structural variables measured were LAI, SD, CC, CD, SH, and ALA.

TABLE II
BANDS AND VEGETATION INDICES OF LANDSAT-8 IMAGERY EXAMINED FOR SLA RETRIEVAL IN THIS STUDY

Band/VI	Description	Wavelength (nm)/ Formulation
B1	Coastal aerosol	435–451 (443)
B2	Blue	452–512 (482)
B3	Green	533–590 (561.5)
B4	Red	636–673 (654.5)
B5	Near infrared (NIR)	851–879 (865)
B6	Short wave infrared (SWIR) 1	1566–1651 (1608.5)
B7	Short wave infrared (SWIR) 2	2107–2294 (2200.5)
EVI	Enhanced vegetation index	$2.5 \left[\frac{\text{NIR} - \text{Red}}{\text{NIR} + 6(\text{Red}) - 7.5(\text{blue}) + 1} \right]$
MSAVI	Modified soil-adjusted vegetation index	$\left(\frac{(\text{NIR} - \text{Red})(1 + L)}{\text{NIR} + \text{Red} + L} \right)$
NBR	Normalized burn ratio	$(\text{NIR} - \text{SWIR2})/(\text{NIR} + \text{SWIR2})$
NBR2	Normalized burn ratio2	$(\text{SWIR1} - \text{SWIR2})/(\text{SWIR1} + \text{SWIR2})$
NDMI	Normalized difference moisture index	$(\text{NIR} - \text{SWIR1})/(\text{NIR} + \text{SWIR1})$
NDVI	Normalized difference vegetation index	$(\text{NIR} - \text{Red})/(\text{NIR} + \text{Red})$
SAVI	Soil-adjusted vegetation index	$\left(\frac{\text{NIR} - \text{Red}}{\text{NIR} + \text{Red} + L} \right) (1 + L)$

Here, L is a correction factor (1, 0.5, and 0.25 for low, intermediate, and high vegetation, respectively).

offset between Landsat 7 and Landsat-8 coverage of each WRS-2 path. The OLI sensor collects image data for nine shortwave spectral bands over a 190-km swath with a 30-m spatial resolution for all bands except the 15-m panchromatic band (see Table II). OLI has an uncertainty of less than 5% in terms of absolute at-aperture spectral radiance and an uncertainty of less than 3% in terms of top-of-atmosphere spectral reflectance for each of the spectral bands (<http://landsat.usgs.gov/l8handbook.php>).

In order to assess the predictive accuracy of SLA from Landsat imagery, the Landsat-8 OLI image of the study area (path 192 and row 26) acquired on 08 August 2013 was utilized. The Landsat surface reflectance image was downloaded from the Global Visualization Viewer (GloVis, <http://glovis.usgs.gov/>) developed by the Earth Resource Observation and Science Centre of the USGS. It contains the surface reflectance data, which have been corrected for systematic radiometric and geometric errors. We ensured the overall geometric accuracy with ground control points and a digital elevation model. Vegetation indices products were also directly downloaded and utilized for SLA estimation. The spatial resolution of Landsat-8 OLI image approximates the size of the sample plots (approximately 30 × 30 m).

The reflectance values of the sample plots were extracted from the Landsat-8 scene and used for further analysis (hereafter, it is referred to as the measured reflectance).

C. SLA Retrieval Approaches

SLA was retrieved using two approaches: 1) developing prediction models using Landsat-8 surface reflectance including individual spectral bands and derived vegetation indices, and 2) inverting invertible forest reflectance model (INFORM) RTM through CWA and a LUT.

1) Prediction Models on Landsat-Spectral Bands and Vegetation Indices: To investigate the prediction of SLA, we utilized seven spectral bands of Landsat-8 located in the visible and NIR regions as well as seven vegetation index (VI) products available directly from the USGS archive in order to predict SLA (see Table II). The performances of each spectral band and VI were evaluated using the coefficient of determination (R^2), root-mean-square error (RMSE), and bias values for the relationship between measured and estimated SLA through cross validation. For this, a wide variety of regression models, such as linear, stepwise linear, multiple linear, and quadratic regressions, were

examined. Predictive models with good fit (i.e., a high R^2 and low RMSE combination during cross validation) were then used to retrieve SLA.

2) RTM Inversion:

a) *Model parameterization and forest reflectance simulation:* To simulate the spectral properties of the test site, we used ‘‘INFORM’’ [26], [27], which is a hybrid RTM that combines the forest light interaction model [28] and SAIL [29] canopy RTMs with the PROSPECT [30] leaf RTM. In INFORM, LAI is represented by the leaf area indices of single trees (LAI_s). Hence, the *in-situ* ground reference values for LAIs were computed from LAI and CC.

$$LAI_s = \frac{LAI}{CC} \quad (1)$$

where LAI_s is a single tree leaf area index and CC is a canopy closure. The model uses several canopy structural and biochemical variables and sensor configuration input parameters to generate the top of forest canopy reflectance. The input parameters include leaf biochemical variables, such as leaf chlorophyll content (C_{ab}), leaf dry matter content per area (C_m), and leaf water content per leaf area (C_w), canopy structural parameters, such as LAI_s , SH, SD, CD, and average leaf angle (ALA), and geometrical parameters, such as sensor zenith, azimuth, and view angles. SLA was computed as the inverse of C_m (see Ali *et al.* [25] for further details).

The INFORM model was run in forward mode to generate a simulated dataset. Next, the CWA was applied on the simulated data to identify spectral (wavelet) features sensitive to SLA. Then, prediction models were developed using the identified wavelet features. To achieve this, the input parameters of INFORM (C_{ab} , C_m , C_w , N , LAI_s , SD, SH, CD, and ALA) were randomly varied 10 000 times, using a multivariate normal distribution function from the field data. To avoid extreme values and unrealistic combinations, the randomly assigned value of each variable was limited to $\pm 5\%$ of the observed maximum and minimum values for that variable in the field data. A random Gaussian noise value of 0.3% [31] was added to each simulated spectrum to account for model uncertainties as well as reduce collinearity between the spectrum and input variables. The simulation was performed for the seven spectral bands corresponding to the band settings of the Landsat-8 surface reflectance data.

A sensitivity study had previously reported an insignificant effect of solar zenith and azimuth angles on INFORM-simulated canopy reflectance [32]. Therefore, other canopy, and external input parameters were fixed, based on the field data and Landsat-8 OLI specifications. Accordingly, values of 0.1 $m^2 m^2$ for understory LAI, 32° for sun zenith angle, 0° for observation zenith angle, and 153° for azimuth angle were used. The fraction of diffused radiation was fixed based on previous study by Schlerf and Atzberger [26]. As bare soil occurred extremely rarely, the field spectra of understory vegetation and the forest floor elements were averaged and used as a fixed background reflectance during the simulation. The fixed background reflectance was obtained by averaging spectral reflectance of understory vegetation and ecosystem elements on the forest floor, such as bark, litter, mosses, and lichens, which were measured

by using the ASD field spectroradiometer coupled to a high-intensity contact probe during the field campaign. For the details on model input parameters used during INFORM parametrization, see Ali *et al.* [20].

b) *RTM inversion using a LUT approach:* RTM inversion using LUT is one of the most popular and efficient methods in remote sensing [15], [21], [33]–[36]. It involves repeated simulation of spectra, using different combinations of model input parameters constrained by reasonable ranges. An LUT of 150 000 forest canopy reflectance spectra was generated by running INFORM in forward mode for Landsat-8 bands and using the prior information on the ranges of input parameters presented in Table I. The inversion was performed by searching for the simulated spectra in the LUT which best fit the measured spectra (Landsat-8 surface reflectance) and retrieving their corresponding SLA. The search for the best fit between simulated and measured spectra was determined by calculating and finding the lowest RMSE of an unconstrained nonlinear multivariate function [37] as shown in (2). The search for the best fit was performed using different spectral band subsets

$$M_N = \sqrt{\frac{\sum_{\lambda} [(\rho_{mes} - \rho_{sim})]^2}{n}} \quad (2)$$

where n is the number of wavelengths, ρ_{mes} and ρ_{sim} are measured and simulated values of reflectance, respectively, and λ is the wavelength.

D. Validation

The prediction performance of the three methods utilized in this study (i.e., statistical, RTM inversion using CWA, and RTM inversion by LUT) was evaluated using R^2 , RMSE %, and bias between estimated and measured values of SLA. The results of the statistical methods were validated by using the measured dataset in a leave-one-out cross-validation procedure in which the calibration set of $n-1$ samples was used to fit the predictive model and then evaluated using the sample that had been left out.

The predictive performances of the RTM inversions were assessed using SLA values collected in 33 sample plots in the field. R^2 , RMSE (%), and bias were calculated as

$$R^2 = 1 - \frac{\sum (y_i - y'_i)^2}{\sum (y_i - \bar{y}_1)^2} \quad (3)$$

$$RMSE (\%) = \sqrt{\frac{\sum (y_i - y'_i)^2}{n}} / \bar{y}_1 * 100 \quad (4)$$

$$Bias = \frac{\sum (y_i - y'_i)}{n} \quad (5)$$

where y_i and y'_i are the actual and predicted values for sample i , and \bar{y}_1 is the arithmetic mean of the measured data, and n is the number of samples in the measured data.

TABLE III
ACCURACY OF THE ESTIMATES OF SLA (DEPENDENT VARIABLE) IN THE BAVARIAN FOREST NATIONAL PARK OBTAINED USING LANDSAT-8 BANDS AND VEGETATION INDICES (INDEPENDENT VARIABLE)

Band/VI	Cross validation		Linear regression equation
	R^2	RMSE (%)	
B1	0.33	8.41	$Y = 0.0039x + 1.2434$
B2	0.16	8.59	$Y = 0.0041x + 1.0657$
B3	0.59	6.46	$Y = 0.0037x + 0.5648$
B4	0.26	8.30	$Y = 0.0035x + 0.9996$
B5	0.74	4.81	$Y = 0.000258x + 1.1897$
B6	0.73	4.95	$Y = 0.000477x + 1.3448$
B7	0.71	5.26	$Y = 0.0011x + 1.3325$
EVI	0.77	4.44	$Y = 0.00014328x + 1.2009$
MSAVI	0.76	4.45	$Y = 0.0001335x + 1.2894$
NBR	0.12	8.29	$Y = 0.0001851x + 3.1924$
NBR2	0.60	6.02	$Y = 0.0008962x + 1.6702$
NDMI	0.32	7.45	$Y = -0.0002417x + 2.8991$
NDVI	0.73	4.68	$Y = 0.0004291x + 1.6476$
SAVI	0.76	4.48	$Y = 0.0007401x + 1.0922$

The accuracy is assessed on the basis of the logarithmic value of SLA. The band and index with high cross validation R^2 and low RMSE are shown in bold.

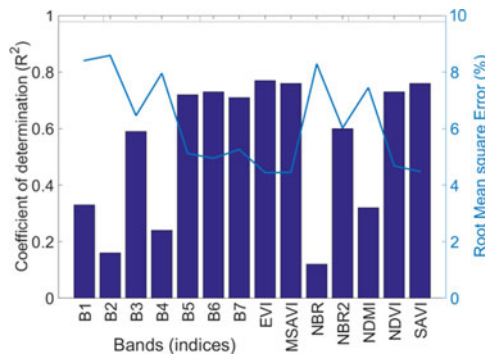


Fig. 1. Cross validated R^2 and RMSE combinations of the Landsat-8 bands and vegetation indices.

III. RESULTS AND DISCUSSION

A. SLA Retrieval Using Landsat-8 Vegetation Indices and Bands

The validation of prediction models developed with individual spectral bands as well as vegetation indices of Landsat-8 surface reflectance data revealed significant correlations with SLA (see Table III). Among the selected seven bands of Landsat-8, the NIR (band 5) and the SWIR (band 6 and band 7) showed stronger correlation to SLA than bands from the visible region. This is in line with previous studies that reported wavelengths in the visible region (400–800 nm) being highly sensitive to leaf pigments, such as chlorophylls and carotenoids, while the NIR and SWIR regions are the most sensitive regions for retrieving parameters related to dry matter, such as SLA [19], [38], [39].

Many of the vegetation indices examined performed well in retrieving SLA from Landsat-8 imagery. In general, combinations of higher R^2 and lower RMSE values were observed at longer wavelengths and VIs, as illustrated in Fig. 1.

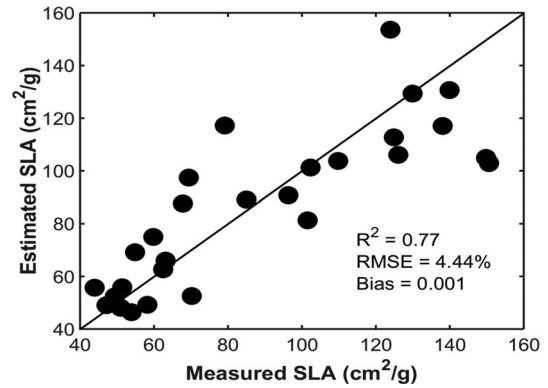


Fig. 2. Measured SLA and SLA estimated using the Landsat-8 EVI-VI. The solid line shows the 1:1 relationship between predicted and measured values of SLA.

The highest R^2 (0.77) and the lowest RMSE (4.44%) combination was recorded for the EVI. The modified soil-adjusted vegetation index (MSAVI) and the soil-adjusted vegetation index (SAVI) were also showed good performance. This reveals the potential of EVI, MSAVI, and SAVI for fast and accurate retrieval of SLA from Landsat-8 imagery. These indices have also previously been shown to be a suitable index for other vegetation parameters e.g., [40], [41].

The precision of the EVI-retrieved SLA against ground-measured SLA is illustrated in Fig. 2. Generally the errors seem randomly distributed throughout the observation with bias close to zero but there is a tendency to under estimate higher values of SLA. One possible explanation for this might be that compared with forest leaves with low SLA values, forest leaves with higher SLA are more transparent, and, therefore, influenced by background material. The other cause might be model saturation. The model might become insensitive to high SLA and contribute to the under estimation of higher values.

B. Inversion of RTM Through Wavelet Analysis

In this approach, SLA was retrieved from Landsat-8 data by applying predictive models developed from INFORM-simulated spectra. Fig. 3(a) illustrates the correlation between the seven bands of Landsat-8 and SLA variation at different scales of wavelet transformation. The wavelengths centred at 561.5, 654.5, and 2200.5 nm showed higher correlation to SLA at scales of 10, 9, and 2, respectively (see Fig. 3) and were selected to develop predictive models. The highest correlation is observed for the wavelet feature 561.5 nm, scale 10. The significant correlation observed between wavelet features and SLA has important implications for developing rigorous inversion algorithms using satellite imageries for fast and accurate estimation of SLA through RTM and wavelet analysis approach.

We developed and evaluated predictive models for SLA estimation using the three selected wavelet features and their possible combinations as predictor variable. The validation results for the simulated and measured Landsat-8 datasets are presented in Table IV. The linear prediction model developed using a combination of wavelet features 654.5 nm, scale 9 and 2200.5 nm,

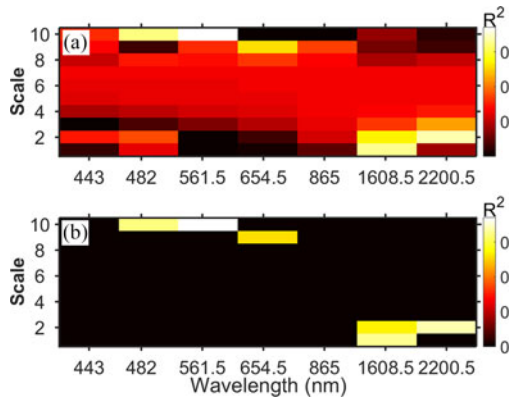


Fig. 3. Correlation scalogram derived from CWA of the simulated spectra for the identification of wavelet features which correlate significantly with SLA. Brightness (a) represents the coefficient of determination (R^2) relating wavelet power to SLA. A colored feature region in scalogram (b) indicates the wavelet features with the top 1% highest R^2 values.

TABLE IV
PERFORMANCE OF THE HIGHLY CORRELATED WAVELET FEATURES IDENTIFIED USING INFORM-SIMULATED SPECTRA AND VALIDATED USING WAVELET FEATURES FROM LANDSAT-8 DATA

No.	Wavelet feature	Calibration		Validation	
		R^2	RMSE (%)	R^2	RMSE (%)
A	561.5 nm, scale 10	0.78	3.66	0.65	5.97
B	654.5 nm, scale 9	0.52	5.43	0.69	11.73
C	2200.5 nm, scale 2	0.71	4.21	0.78	13.25
D	Combination of A and B	0.88	2.67	0.71	9.80
E	Combination of A and C	0.79	3.64	0.61	6.94
F	Combination of B and C	0.78	3.68	0.79	7.52
G	Combination of A, B, and C	0.84	3.17	0.70	27.44

scale 2 showed the highest R^2 (0.79) with the Landsat-8 data (validation). Higher R^2 and lower RMSE combinations were largely perceived in the simulated data. RMSEs were higher in the measured (Landsat-8) dataset than in the simulated dataset. This may be partly explained by mismatch between the simulated and measured datasets, which could have caused the values of the wavelet features obtained from Landsat-8 wavelet analysis to exhibit systematic shifts to higher or lower values, resulting in systematic overestimation of SLA (see Fig. 4). A study by Ali *et al.* [20] using hyperspectral airborne data reported a similar problem and suggested that the probable causes of this shift were atmospheric effects and sensor noise on the measured spectra. These factors may cause variation in local absorption peaks on the measured spectra, and lead to higher or lower wavelet power values during the transformation.

C. Inversion of RTM by a LUT Approach

Inversion of the INFORM model via a LUT, and all the Landsat-8 spectral bands yielded a high R^2 (0.84) value for SLA. However, the scatter plot of measured and estimated SLA values does not follow a one-to-one relationship line (see Fig. 5(a)), and the RMSE was relatively high (8.02%). This may be due to poor correlation of the VIS region bands with SLA.

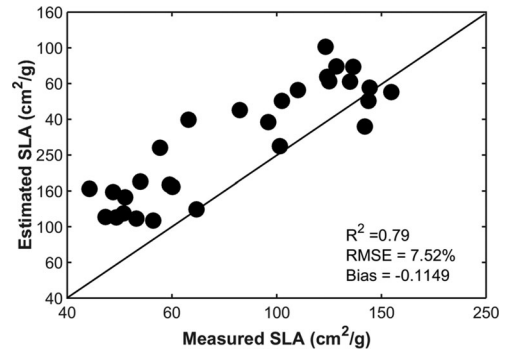


Fig. 4. Measured and estimated SLA using a combination of the two wavelet features (654.5 nm, scale 9 and 2200.5 nm, scale 2) as predictor variables. The solid line shows the 1:1 relationship between predicted and measured values of SLA.

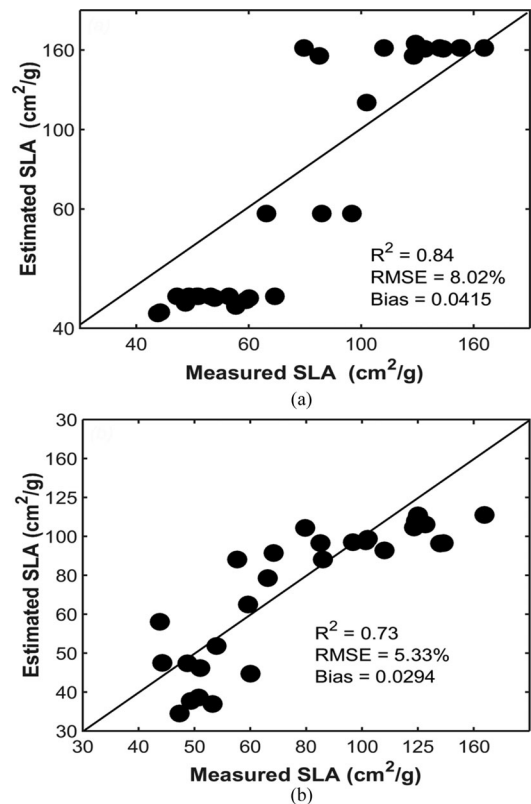


Fig. 5. Scatter plot of measured SLA and SLA estimated using the LUT. Validation results from inversion (a) using all seven bands listed in Table II, and (b) validation results from inversion using bands 5, 6, and 7. The solid line shows the 1:1 relationship between the predicted and measured values of SLA.

The latter was further investigated by performing the inversion using a spectral subset. The spectral subset was chosen from the bands that earlier (see Section III-B) showed good performance in the empirical method (i.e., bands 5, 6, and 7). Consequently, when inversion was performed using these bands, the relationship between measured and estimated SLA became stronger and demonstrated a lower RMSE (5.33%). This spectral subset (bands from the NIR and SWIR regions) yielded a more precise result than any other spectral subset (not shown). The estimated and measured SLA values using this subset appeared to follow a one-to-one relationship in the scatter plot

(see Fig. 5(b)). One of the main reasons could be that there was low error (mismatch) between the simulated and measured reflectance in those spectral bands. Our results confirm those of a study by Darvishzadeh *et al.* [34]; those authors recommended inverting RTM by LUT based on a spectral subset that has a low average absolute error between simulated and measured spectral reflectance.

In general, validation of the two approaches (i.e., statistical and RTM inversion) showed similar accuracies for SLA retrieval. During validation, slightly higher R^2 (0.79–0.88) was recorded in the RTM inversion than in the statistical approach (maximum $R^2 = 0.77$), but the lowest RMSE (4.44%) was obtained in the statistical approach when using the VI-EVI. Our findings are in agreement with those of Lymburner *et al.* [16], who tested several existing vegetation indices in order to estimate forest SLA from Landsat TM imagery and found a strong correlation ($R^2 \geq 0.74$) between average canopy SLA and vegetation indices of Landsat TM data, such as the soil and atmosphere resistant vegetation index, the NDVI, and the ratio vegetation index. However, it is worth noting that using vegetation indices is highly site and sensor specific. A strong correlation between leaf mass per area and reflectance in the 750- to 2500-nm wavelength range has also been reported for tropical rainforest leaf samples [38], [42]. However, in our study, the accuracy of both statistical and RTM-based SLA retrieval from Landsat-8 data was lower than the accuracy of SLA retrieved from hyperspectral data; Ali *et al.* [17] reported higher accuracy ($R^2 = 0.88$ and RMSE = 3.34%) when retrieving SLA using optimized soil-adjusted vegetation index from HySpex imagery. Inversion of RTM through CWA on HySpex was also higher ($R^2 = 0.85$ and RMSE = 4.90%) [20] than in this study ($R^2 = 0.79$ and RMSE = 7.52%). Nevertheless, the results of this study revealed the potential of multispectral satellites, in particular of the new generation of satellites, such as Landsat-8 and Sentinel-2, for retrieving SLA particularly in the NIR and SWIR regions.

IV. CONCLUSION

The main goal of this study was to evaluate the potential of Landsat-8 imagery to retrieve SLA by using either statistical (empirical) or physical (RTM) approaches. In the retrieval process, both statistical and RTM approaches showed good performance. However, systematic errors were observed in the inversion of RTM through CWA. Typically, the influence of upscaling to coarser remote-sensing data (satellite image) on retrieval accuracy was minimal. The evidence from this study suggests that one can apply simple statistical methods such as the EVI for fast and reasonable mapping of SLA at local scales from spaceborne satellite imagery. However, since the VI tends to be site and sensor specific, a more robust and vigorous approach when temporal mapping of SLA at regional and global scales is required could be RTM inversion. This study has gone some way toward enhancing our understanding of quantifying plant functional traits from remotely sensed data with coarse spectral resolution. However, in this study, the forest area is mainly dominated by three tree species: namely

European beech, Norway spruce, and Fir. Therefore, the application of the developed methods to other structurally different vegetation types and heterogeneous areas with high species variability and vegetation communities need to be evaluated using both hyperspectral and multispectral remote sensing data. Further research is also required to explore the potential of new high- and medium-resolution spaceborne satellite data for accurate retrieval of SLA.

ACKNOWLEDGMENT

The authors would like to thank Dr. H. Heiden, Dr. S. Holzwarth, and Dr. N. Pinnel in the German Remote Sensing Data Center and Dr. H. Latifi in the Institute of Geography and Geology, University of Würzburg, in selecting the test site and facilitating the field campaign. They would also like to thank the Bavarian Forest National Park particularly to Dr. M. Heurich, Dr. J. Mueller, and W. Breit for approving access to the study area, providing the crossbow with its accessories, and other field and logistical facilities. Lastly, they would like to thank Z. Wang and T. Wang in the faculty of Geo-Information Science and Earth Observation, University of Twente, who assisted with the fieldwork design and data collection.

REFERENCES

- [1] A. K. Skidmore *et al.*, "Environmental science: Agree on biodiversity metrics to track from space," *Nature*, vol. 523, pp. 403–405, 2015.
- [2] L. L. Pierce, S. W. Running, and J. Walker, "Regional-scale relationships of leaf-area index to specific leaf-area and leaf nitrogen-content," *Ecolog. Appl.*, vol. 4, pp. 313–321, May 1994.
- [3] C. F. Zhang, Z. Y. Pan, H. Dong, F. J. He, and X. B. Hu, "Remote estimation of leaf water content using spectral index derived from hyperspectral data," in *Proc. 1st Int. Conf. Inf. Sci. Electron. Technol.*, 2015, vol. 3, pp. 20–23.
- [4] X. N. Song, J. W. Ma, X. T. Li, P. Leng, F. C. Zhou, and S. Li, "Estimation of vegetation canopy water content using hyperion hyperspectral data," *Spectrosc. Spectral Anal.*, vol. 33, pp. 2833–2837, Oct. 2013.
- [5] Y. Knyazikhin *et al.*, "Hyperspectral remote sensing of foliar nitrogen content," *Proc. Nat. Acad. Sci. United States Amer.*, vol. 110, pp. E185–E192, Jan. 15, 2013.
- [6] J. Misurec *et al.*, "Utilization of hyperspectral image optical indices to assess the Norway spruce forest health status," *J. Appl. Remote Sens.*, vol. 6, pp. 063545-1–063545-25, Jun. 29, 2012.
- [7] J. G. P. W. Clevers and L. Kooistra, "Using hyperspectral remote sensing data for retrieving canopy chlorophyll and nitrogen content," *IEEE J. Sel. Topics Appl. Earth Obs. Remote Sens.*, vol. 5, no. 2, pp. 574–583, Apr. 2012.
- [8] Z. Wang *et al.*, "Vegetation indices for mapping canopy foliar nitrogen in a mixed temperate forest," *Remote Sens.*, vol. 8, no. 491, pp. 1–20, 2016.
- [9] X. J. She, L. F. Zhang, Y. Cen, T. X. Wu, C. P. Huang, and M. H. A. Baig, "Comparison of the continuity of vegetation indices derived from landsat 8 OLI and landsat 7 ETM+ data among different vegetation types," *Remote Sens.*, vol. 7, pp. 13485–13506, Oct. 2015.
- [10] P. Li, L. G. Jiang, and Z. M. Feng, "Cross-comparison of vegetation indices derived from Landsat-7 enhanced thematic mapper plus (ETM plus) and landsat-8 operational land imager (OLI) sensors," *Remote Sens.*, vol. 6, pp. 310–329, Jan. 2014.
- [11] T. Dube and O. Mutanga, "Investigating the robustness of the new Landsat-8 operational land imager derived texture metrics in estimating plantation forest aboveground biomass in resource constrained areas," *ISPRS J. Photogramm. Remote Sens.*, vol. 108, pp. 12–32, 2015.
- [12] L. Ji *et al.*, "Estimating aboveground biomass in interior Alaska with Landsat data and field measurements," *Int. J. Appl. Earth Obs. Geoinf.*, vol. 18, pp. 451–461, 2012.
- [13] W. Robles, J. D. Madsen, and R. M. Wersal, "Estimating the biomass of waterhyacinth (*eichhornia crassipes*) using the normalized difference vegetation index derived from simulated Landsat 5 TM," *Invasive Plant Sci. Manage.*, vol. 8, pp. 203–211, 2015.

- [14] J. Wang *et al.*, "Estimation of rice phenology date using integrated HJ-1 CCD and Landsat-8 OLI vegetation indices time-series images," *J. Zhejiang Univ.-Sci. B*, vol. 16, pp. 832–844, Oct. 2015.
- [15] X. Tao, S. Liang, T. He, and H. Jin, "Estimation of fraction of absorbed photosynthetically active radiation from multiple satellite data: Model development and validation," *Remote Sens. Environ.*, vol. 184, pp. 539–557, Oct. 2016.
- [16] L. Lyburner, P. J. Beggs, and C. R. Jacobson, "Estimation of canopy-average surface-specific leaf area using Landsat TM data," *Photogramm. Eng. Remote Sens.*, vol. 66, pp. 183–191, Feb. 2000.
- [17] A. M. Ali, R. Darvishzadeh, A. K. Skidmore, and I. V. Duren, "Specific leaf area estimation from leaf and canopy reflectance through optimization and validation of vegetation indices," *Agriculture Forest Meteorol.*, vol. 236, pp. 162–174, 2017.
- [18] G. le Maire *et al.*, "Calibration and validation of hyperspectral indices for the estimation of broadleaved forest leaf chlorophyll content, leaf mass per area, leaf area index and leaf canopy biomass," *Remote Sens. Environ.*, vol. 112, pp. 3846–3864, Oct. 15, 2008.
- [19] A. Romero, I. Aguado, and M. Yebra, "Estimation of dry matter content in leaves using normalized indexes and PROSPECT model inversion," *Int. J. Remote Sens.*, vol. 33, pp. 396–414, 2012.
- [20] A. M. Ali, A. K. Skidmore, R. Darvishzadeh, I. V. Duren, S. Holzwarth, and J. Mueller, "Retrieval of forest leaf functional traits from hypspx imagery using radiative transfer models and continuous wavelet analysis," *Photogramm. Remote Sens.*, vol. 122, pp. 68–80, 2016.
- [21] R. Darvishzadeh, C. Atzberger, A. Skidmore, and M. Schlerf, "Mapping grassland leaf area index with airborne hyperspectral imagery: A comparison study of statistical approaches and inversion of radiative transfer models," *ISPRS J. Photogramm. Remote Sens.*, vol. 66, pp. 894–906, 2011.
- [22] M. Heurich, B. Beudert, H. Rall, and Z. Krenova, "National Parks as model regions for interdisciplinary long-term ecological research," in *Long-Term Ecological Research Between Theory and Application*, F. Müller, C. Baessler, H. Schubert, and S. Klotz, Eds. Dordrecht, The Netherlands: Springer, 2010, pp. 327–344.
- [23] M. Heurich and M. Neufanger, *Die Wälder des Nationalparks Bayerischer Wald: Ergebnisse der Waldinventur 2002/2003 im geschichtlichen und waldökologischen Kontext*. Grafenau, Germany: Nationalparkverwaltung Bayerischer Wald, 2005.
- [24] L. W. Lehnert, C. Bäessler, R. Brandl, P. J. Burton, and J. Müller, "Conservation value of forests attacked by bark beetles: Highest number of indicator species is found in early successional stages," *J. Nature Conserv.*, vol. 21, pp. 97–104, 2013.
- [25] A. M. Ali, R. Darvishzadeh, A. K. Skidmore, I. V. Duren, U. Heiden, and M. Heurich, "Estimating leaf functional traits by inversion of PROSPECT: Assessing leaf dry matter content and specific leaf area in mixed mountainous forest," *Int. J. Appl. Earth Obs. Geoinf.*, vol. 45, Part A, pp. 66–76, Mar. 2016.
- [26] M. Schlerf and C. Atzberger, "Inversion of a forest reflectance model to estimate structural canopy variables from hyperspectral remote sensing data," *Remote Sens. Environ.*, vol. 100, pp. 281–294, Feb. 15, 2006.
- [27] C. Atzberger, "Development of an invertible forest reflectance model: The INFOR-model," in *Proc. 20th Eur. Assoc. Remote Sens. Lab. Symp.*, Dresden, Germany, Jun. 14–16, 2000, pp. 39–44.
- [28] A. Rosema, W. Verhoef, H. Noorbergen, and J. J. Borgesius, "A new forest light interaction-model in support of forest monitoring," *Remote Sens. Environ.*, vol. 42, pp. 23–41, Oct. 1992.
- [29] W. Verhoef, "Light-scattering by leaf layers with application to canopy reflectance modeling—The sail model," *Remote Sens. Environ.*, vol. 16, pp. 125–141, 1984.
- [30] S. Jacquemoud and F. Baret, "Prospect—A model of leaf optical-properties spectra," *Remote Sens. Environ.*, vol. 34, pp. 75–91, Nov. 1990.
- [31] T. Cheng, B. Rivard, A. G. Sánchez-Azofeifa, J.-B. Féret, S. Jacquemoud, and S. L. Ustin, "Deriving leaf mass per area (LMA) from foliar reflectance across a variety of plant species using continuous wavelet analysis," *ISPRS J. Photogramm. Remote Sens.*, vol. 87, pp. 28–38, Jan. 2014.
- [32] A. M. Ali, R. Darvishzadeh, A. K. Skidmore, and I. V. Duren, "Effects of canopy structural variables on retrieval of leaf dry matter content and specific leaf area from remotely sensed data," *IEEE J. Sel. Topics Appl. Earth Obs. Remote Sens.*, vol. 9, no. 12, pp. 898–909, Feb. 2016.
- [33] S. Dasgupta, J. J. Qu, and S. Bhoi, "Constrained radiative transfer inversions for vegetation moisture retrievals in grasslands," *J. Appl. Remote Sens.*, vol. 3, pp. 1–15, 2009.
- [34] R. Darvishzadeh, A. Skidmore, M. Schlerf, and C. Atzberger, "Inversion of a radiative transfer model for estimating vegetation LAI and chlorophyll in a heterogeneous grassland," *Remote Sens. Environ.*, vol. 112, pp. 2592–2604, May 15, 2008.
- [35] V. K. Sehgal, D. Chakraborty, and R. N. Sahoo, "Inversion of radiative transfer model for retrieval of wheat biophysical parameters from broadband reflectance measurements," *Inf. Process. Agriculture*, vol. 3, pp. 107–118, Jun. 2016.
- [36] G. F. Yin *et al.*, "Regional leaf area index retrieval based on remote sensing: The role of radiative transfer model selection," *Remote Sens.*, vol. 7, pp. 4604–4625, Apr. 2015.
- [37] T. F. Coleman and Y. Y. Li, "An interior trust region approach for nonlinear minimization subject to bounds," *SIAM J. Optim.*, vol. 6, pp. 418–445, May 1996.
- [38] G. P. Asner *et al.*, "Taxonomy and remote sensing of leaf mass per area (LMA) in humid tropical forests," *Ecolog. Appl.*, vol. 21, pp. 85–98, Jan. 2011.
- [39] S. Jacquemoud, S. L. Ustin, J. Verdebout, G. Schmuck, G. Andreoli, and B. Hosgood, "Estimating leaf biochemistry using the PROSPECT leaf optical properties model," *Remote Sens. Environ.*, vol. 56, pp. 194–202, Jun. 1996.
- [40] H. Fraga *et al.*, "Examining the relationship between the enhanced vegetation index and grapevine phenology," *Eur. J. Remote Sens.*, vol. 47, pp. 753–771, 2014.
- [41] Q. H. Lin, "Enhanced vegetation index using moderate resolution imaging spectroradiometers," in *Proc. 2012 5th Int. Congr. Image Signal Process.*, 2012, pp. 1043–1046.
- [42] G. P. Asner and R. E. Martin, "Spectral and chemical analysis of tropical forests: Scaling from leaf to canopy levels," *Remote Sens. Environ.*, vol. 112, pp. 3958–3970, 2008.



Abebe Mohammed Ali received the B.Sc. degree (very great distinction) in forestry from Wondo Genet College of Forestry, Debub University, Awasa, Ethiopia, in 2002, the M.Sc. degree in geoinformation science from Wageningen University, Wageningen, The Netherlands, in 2006, and the Ph.D. degree from the Faculty of Geo-Information Science and Earth Observation, University of Twente, Enschede, The Netherlands, in October 6, 2016.

He was a GIS and Remote Sensing Officer from 2007 to 2009. He has been a Lecturer and Head of Geography and Environmental Studies Department, Wollo University, Dessie, Ethiopia, since 2009. His current research interests include development of optical remote sensing approaches and assessing quantitatively the biophysical and biochemical variables of vegetation using radiative transfer models.



Roshanak Darvishzadeh received the Ph.D. degree in hyperspectral remote sensing of vegetation from Wageningen University, Wageningen, The Netherlands, in 2008.

She is currently an Assistant Professor in the Department of Natural Resources, Faculty of Geo-Information Science and Earth Observation, University of Twente, Enschede, The Netherlands. She has ample experience on the use of lab and field instruments and quantitative methods in vegetation mapping and monitoring. Her research interests include mapping and modeling biochemical and biophysical properties of vegetation with the use of statistical and radiative transfer models and exploration of hyperspectral, multispectral, thermal hyperspectral, and LIDAR data.



Andrew K. Skidmore received the Ph.D. degree in remote sensing and GIS from Australian National University, Canberra, A.C.T., Australia, in 1989.

He is currently the Professor of Spatial Environmental Resource Dynamics with the University of Twente, Enschede, The Netherlands and Chairman in the Department of Natural Resources, Faculty of Geo-Information Science and Earth Observation. He has authored more than 190 ISI journal articles and 17 book chapters. His research interests include hyperspectral remote sensing, habitat monitoring under fragmentation and climate change, as well as image processing and more generally techniques for handling geoinformation.